Nanoscale

Accepted Manuscript

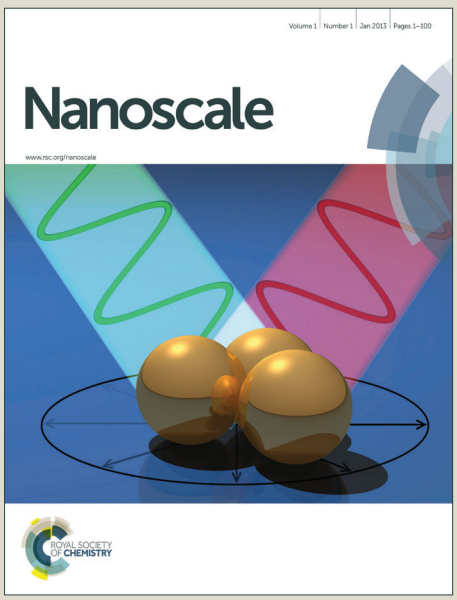

ROYAL SOCIETY OF CHEMISTRY

www.rsc.org/nanoscale

Cite this: DOI: 10.1039/c0xx00000x

www.rsc.org/xxxxxx

PAPER

A WS_2 nanosheet based sensing platform for highly sensitive detection of T4 polynucleotide kinase and its inhibitors

Jia Ge, Li-Juan Tang, Qiang Xi, Xi-Ping Li, Ru-Qin Yu*, Jian-Hui Jiang, and Xia Chu*

Received (in XXX, XXX) Xth XXXXXXXXX 20XX, Accepted Xth XXXXXXXXX 20XX
DOI: 10.1039/b000000x

DNA phosphorylation, catalyzed by polynucleotide kinase (PNK), plays significant regulatory roles in many biological events. Here, a novel fluorescent nanosensor based on phosphorylation-specific exonuclease reaction and efficient fluorescence quenching of single-stranded DNA (ssDNA) by WS_2 nanosheet has been developed for monitoring the activity of PNK using T4 polynucleotide kinase (T4 PNK) as a model target. The fluorescent dye-labeled double-stranded DNA (dsDNA) remains highly fluorescent when mixed with WS_2 nanosheets because of the weak adsorption of dsDNA on WS_2 nanosheets. While dsDNA is phosphorylated by T4 PNK, it can be specifically degraded by λ exonuclease, producing ssDNA strongly adsorbed on WS_2 nanosheets with greatly quenched fluorescence. Because of the high quenching efficiency of WS_2 nanosheets, the developed platform presents excellent performance with a wide linear range, low detection limit and high signal-to-background ratio. Additionally, inhibition effects from adenosine diphosphate, ammonium sulfate, and sodium chloride have been investigated. The method may provide a universal platform for PNK activity monitoring and inhibitor screening in drug discovery and clinic diagnostics.

Introduction

Phosphorylation of DNA by polynucleotide kinase (PNK) takes an crucial role in a majority of normal cellular events, such as nucleic acid metabolism, DNA damage repair, DNA replication and DNA recombination.[1-3] T4 polynucleotide kinase (T4 PNK), first discovered in 1965,[4] is a bifunctional enzyme possessing the capacity to phosphorylate DNA at 5'-hydroxyl termini by catalyzing the transfer of the λ-phosphate residue of ATP to nucleic acids and oligonucleotides.[5,6] T4 PNK plays an important role in detection of DNA adducts or oligonucleotides, nucleic acid metabolism, and repair of DNA lesions.[7-10] On account of the significance of PNK, the development of assays for PNK activities is therefore of fundamental importance.

There have been several methods for the detection of phosphorylation and activity of DNA kinase, including radioisotope ^{32}P-labeling, polyacrylamide gel electrophoresis (PAGE), autoradiography and fluorescence.[4, 11, 12] However, these methods have the shortcomings of being time consuming, laborious, not sensitive, or requiring the radiolabeling of substrates. Therefore, alternative assay methods circumventing the afore-mentioned problems need to be explored for the investigation of the phosphorylation of nucleic acids. Tang et al. described a fluorescence assay using molecular beacon DNA probes to investigate the phosphorylation process of nucleic acids by T4 PNK.[13] Song and Zhao described a novel method for real time monitoring of the activity and kinetics of T4 PNK by use of a singly fluorophore-labeled molecular beacon DNA probe coupled with λ exonuclease cleavage.[14] However, design of specific dye-labeled molecular beacon DNA is difficult and costly. Thus, the development of more sensitive and convenient methods for T4 PNK assay is still required.

Two-dimensional nanomaterials have received much attention in recent years owing to their unusual quantum properties and surface effect. Graphene is a successful example 2D carbon material, exhibiting exceptional physical properties such as a high electron conductivity and excellent mechanical strength.[15] Hence, graphene has attracted significant research interest and hold great potential for many applications.[16-22] WS_2 nanosheets are archetypical examples of inorganic analogues of graphene, the layer of a WS_2 is three atoms thick with the composition of hexagonal layer of metal atoms W sandwiched between two layers of chalcogen atoms.[23, 24] Compared with graphene, WS_2 nanosheets can be synthesized in large scale, and can be directly dispersed in aqueous solution, implying that WS_2 nanosheets will hold great promise as a novel nanomaterial for biomedical applications. Nevertheless, the use of WS_2 nanosheets as a bioanalytical platform has largely unexplored. In addition, most transition-metal ions possess intrinsic fluorescence quenching properties.[25] It has been reported that graphene oxide

(GO) can bind and quench fluorescent dye-labeled single-stranded DNA (ssDNA) probes, while it has less affinity toward double-stranded DNA (dsDNA) or secondary and tertiary structured DNA.[19, 26] We for the first time found that WS_2 nanosheets also have the similar property of spontaneously adsorbing fluorescent dye-labeled ssDNA by the van der Waals force between nucleobases and the basal plane of WS_2 nanosheets, and acting as an efficient fluorescent dye quencher.

Herein, we describe a simple but universal WS_2 nanosheets platform, with T4 PNK as a model, for analysis of nucleotide kinase activity and its inhibition by λ exonuclease cleavage reaction as well as the fluorescence resonance energy transfer (FRET) between fluorescent dye-labeled ssDNA and WS_2 nanosheets. The λ exonuclease is a highly processive 5'-3' dsDNA exonuclease, which digests dsDNA with a phosphate moiety at 5'-ends and has very low activity on non-phosphorylated DNA. Sensitive detection of T4 PNK activity and inhibitor screening were achieved due to the excellent fluorescence quenching ability of WS_2 nanosheets and the efficient cleavage of dsDNA with 5-phosphoryl termini by λ exonuclease. In presence of WS_2 nanosheets, fluorescent dye-labeled dsDNA exhibits strong fluorescence emission, while quite low fluorescence signal is observed when the phosphorylated double helixes are cleaved by λ exonuclease, providing a high signal-to-background ratio. In addition, much simpler than the hairpin DNA probe design, the design of the aforementioned DNA probe in our experiments is not strictly limited. Compared to the traditional methods, the asproposed strategy is convenient but with high analytical performance. The method is not only meaningful for further research on the disease-related biochemical process but also valuable to the molecular-target therapies and the nucleotide kinase-target drug discovery.

Experimental Procedures

Materials

The DNA sequences used in this work were synthesized by Shanghai Sangon Biological Engineering Technology & Services Co., Ltd. The sequences of the DNA oligonucleotides were as follows:

P1: 5'-FAM - CATAGCGGCAGGATCAGTTACAGTG-3'

P2: 5'-CACTGTAACTGATCCTGCCGCTATG-3'

WS_2 nanosheets were prepared according to Voiry method.[27] T4 polynucleotide kinase (10 units/μL), λ exonuclease (5 units/μL), apurinic/apyrimidinic endonuclease 1 (APE 1), cAMP-dependent protein kinase (PKA) and Uracil-DNA Glycosylase (UDG) were obtained from New England Biolabs (NEB, U.K.). Adenosine triphosphate (ATP), dithiothreitol (DTT), PDGF-BB human, lysozyme (41800 U/mg), and adenosine diphosphate (ADP) were bought from Sigma-Aldrich (Shanghai, China). All reagents were used as received without further purification. All solutions were prepared using ultrapure water, obtained through a Millipore Milli-Q water purification system (Billerica, MA, USA) having an electric resistance >18.2 MΩ.

The fluorescence measurements were carried out on an FL-7000 spectrometer (Hitachi, Japan). The fluorescence emission spectra were collected from 500 nm to 600 nm at room temperature with a 488 nm excitation wavelength.

DNA Hybridization and Fluorescence Quenching Assay

In order to prepare FAM labeled dsDNA, P1 and P2 were dissolved in enzymatic reaction buffer and diluted to the desired concentration. Two ssDNA probes were mixed together and then the mixture was denatured at 95 ℃ for 10 min, and cooled slowly to room temperature. To evaluate the fluorescence quenching of P1 and FAM labeled dsDNA on the WS_2 nanosheets surface, 100 nM P1, and 100 nM FAM labeled dsDNA were prepared in the reaction buffer (70 mM Tris-HCl, 10 mM $MgCl_2$, 5 mM DTT, pH 8.0) containing 10 units of λ exonuclease. After the addition of WS_2 nanosheets (0.025 mg/mL), the fluorescence of the mixture was measured at 520 nm with the excitation of 488 nm at room temperature.

Phosphorylation of T4 PNK-catalyzed and Optimization of Assay Conditions

In a typical phosphorylation and cleavage assay, 100 nM FAM labeled dsDNA, 0.5 mM ATP, 10 units of λ exonuclease, and a certain amount of T4 PNK were put into 100 μL of reaction buffer. After the incubation at 37 ℃ for 30 min, 20 μL WS_2 nanosheets (0.025 mg/mL) was added into the reaction mixture, followed by the fluorescence measurement with the excitation wavelength of 488 nm. The optimizations of λ exonuclease concentration, ATP concentration, and phosphorylation time, respectively.

Kinase Inhibitor Evaluation

In the inhibition experiment, to evaluate the effects of inhibitors on the phosphorylation process of T4 PNK-catalyzed, several kinds of inhibitors, including ADP, $(NH_4)_2SO_4$, and NaCl, were contained in the reaction buffer, respectively. After the addition of 100 nM dsDNA, 0.5 mM ATP, 10 units of λ exonuclease, and T4 PNK (10 U mL^{-1}), the reaction was performed at 37 ℃ for 30 min. The following procedures were similar as above.

T4 PNK Activity Detection in Diluted Cell Extracts

Hela cells were cultured in RPMI 1640 medium supplemented with 12% fetal calf serum, 100 μg mL^{-1} streptomycin, and 100 units mL^{-1} penicillin. Cell extracts were prepared according to the previous reports.[28] The collected cells were resuspended in 20 μL 10 mM Tris-HCl (pH 7.8) containing 150 mM NaCl. Into the suspension equal volume of lysis buffer was added which contained 10 mM Tris-HCl (pH 7.8), 150 mM NaCl, 2 mM EDTA, 2 mM DTT, 40% glycerol, 0.2% NP40, and 0.4 mM phenylmethylsulfonyl fluoride. The mixtures were incubated for 1 h at 4 ℃ with occasional shake. Cell debris was removed by centrifugation at 10000 rpm for 10 min, and the supernatant was recovered. Diluted cell extracts were added to the assay solution (1%). The detection procedure was the same as those described in the aforementioned experiment for T4 PNK detection in clean reaction buffer.

Results and Discussion

Strategy for T4 PNK Activity Detection

The developed strategy for investigating T4 PNK activity is demonstrated in Scheme 1. FAM labeled dsDNA acting as a sensitive signal report probe, was obtained by hybridization between the probe 1 labeled with FAM (P1) and probe 2 (P2). After phosphorylation of FAM labeled dsDNA by T4 PNK in the presence of ATP, λ exonuclease would digest dsDNA immediately, and the fluorescence of dsDNA was substantially quenched after mixing with a certain amount of WS_2 nanosheets. On the contrast, in the absence of T4 PNK, 5'-end of dsDNA retained a hydroxyl group, prohibiting the digestion. So, no obvious fluorescence decrease was observed after mixing with the same amount of WS_2 nanosheets. Two reasons play the key role in this type of sensing design. First, λ exonuclease is a highly processive 5' to 3' dsDNA exonuclease, which digests dsDNA with a phosphate moiety at 5'-ends and has very low activity on non-phosphorylated DNA. Second, the adsorption of non-phosphorylated FAM labeled dsDNA at the WS_2 nanosheet surface is weak and unstable. Nevertheless, when the FAM labeled dsDNA was phosphorylated by T4 PNK at the 5'-hydroxyl end, the resulting 5'-phosphoryl termini product was then promptly cleaved by λ exonuclease, yielding a FAM labeled ssDNA. The fluorescence was greatly quenched after the addition of WS_2 nanosheets originated from the strong adsorption of ssDNA on WS_2 nanosheets surface and the effective FRET between the fluorescent dye and WS_2 nanosheets. Thus the activity of T4 PNK can be easily reflected by the fluorescence signals change.

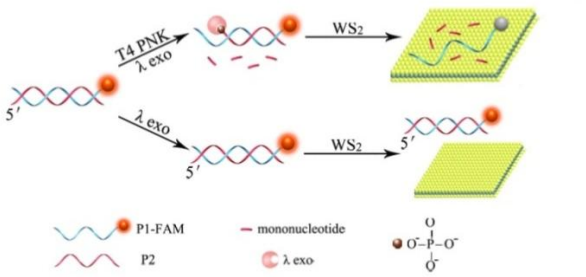

Scheme 1. Schematic representation of WS_2 nanosheets-based platform for T4 PNK activity and inhibition analysis.

Characterization of WS_2 Nanosheets

WS_2 nanosheets prepared according to Voiry method[27] were characterized by transmission electron microscopy (TEM), atomic force microscopy (AFM), and X-ray diffraction (XRD). AFM characterization of the as-prepared WS_2 nanosheets indicated that the thickness of the nanosheets was ~1.8 nm, evidencing the successful synthesis of the two-layer WS_2 nanosheets (Fig.1A). Stable dispersions of WS_2 nanosheets were obtained in aqueous solutions, no sediment observed even after the WS_2 nanosheets were stored for more than one week (Fig. 1B). A negative ζ potential of -17 mV was observed for the nanosheets (Fig. S1 in ESI), indicating a negative charge on the WS_2 nanosheet surfaces. XRD patterns revealed that there was no (002) reflection for the nanosheets (Fig. 1C).

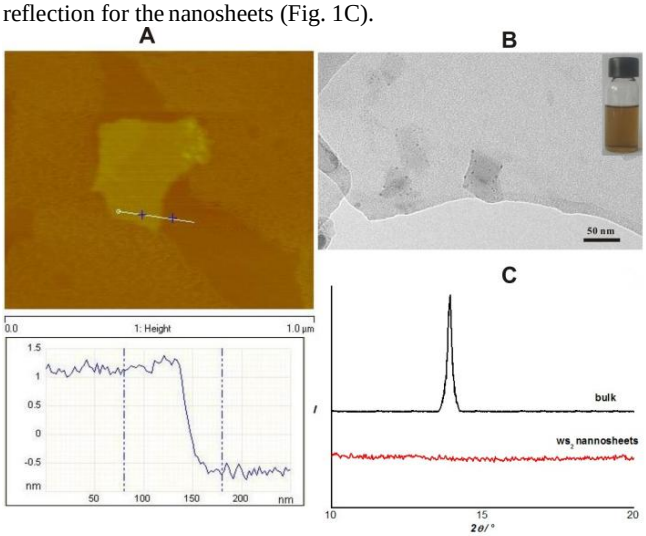

Fig. 1. (A) Typical AFM image of the prepared WS_2 nanosheets. (B) Typical TEM image of prepared WS_2 nanosheets and photograph of a typical chemically exfoliated WS_2 suspension in water. (C) Comparison of XRD patterns of bulk WS_2 and WS_2 nanosheets.

Interactions between FAM Labeled DNA and WS_2 Nanosheets

Fluorescence emission spectra are used to investigate the fluorescence quenching of fluorescent dye resulting from the interaction between FAM labeled DNA and WS_2 nanosheets. It is observed from Fig. 2a, P1 exhibited strong fluorescence emission around 520 nm in the absence of WS_2 nanosheets. However, up to 95% fluorescence emission was quenched upon the addition of 20 μL of WS_2 nanosheets (Fig. 2d). The fact is attributed to the strong adsorption of the ssDNA on the WS_2 nanosheet surface and the super fluorescence quenching ability of WS_2 nanosheets originated from the effective FRET between the fluorescent dye and WS_2 nanosheets. While, as a comparison, 96% fluorescence still remained when FAM labeled dsDNA was mixed with WS_2 nanosheets under the same experimental conditions (Fig. 2c). It is mainly due to the weak and unstable adsorption of FAM labeled dsDNA on the WS_2 nanosheet surface, which inhibited the FRET between the fluorescent dye and WS_2 nanosheets.

The kinetic behaviors of the newly designed WS_2 nanosheets platform were studied by monitoring the fluorescence intensity as a function of time. The adsorption of P1 on the surface of WS_2 nanosheet is very fast at room temperature (Fig. S2, curve a in ESI). The process of adsorption reaches equilibrium within 5 min. However, the FAM labeled dsDNA has much lower binding ability to WS_2 nanosheets, as observed in the time dependent experiments. For FAM labeled dsDNA, WS_2 nanosheets could not cause a remarkable fluorescence decrease within 30 min (Fig. S2, curve b in ESI). This phenomenon can be explained by the difference in absorption between ssDNA and dsDNA at the WS_2 nanosheets.

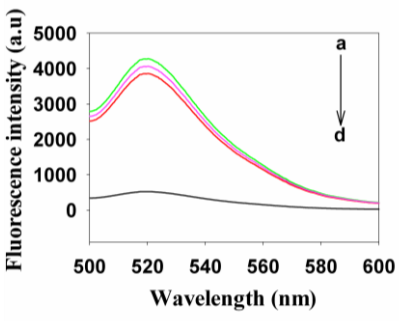

Fig. 2. Fluorescence spectra of 100 nM P1 without (a) and with (d) incubation with 20 μL WS_2 nanosheets in Tris-HCl buffer. Fluorescence spectra of 100 nM FAM labeled dsDNA after incubation without (b) and with (c) 20 μL WS_2 nanosheets in Tris-HCl buffer.

Monitoring of the T4 PNK-Catalyzed Phosphorylation

Fig. 3 indicated the fluorescence emission of FAM labeled dsDNA after the coupled enzymatic reaction with (curve a) and without (curve b) T4 PNK using WS_2 nanosheets as a sensing platform. As shown in Fig. 3, in the absence of T4 PNK, FAM labeled dsDNA exhibits high fluorescence signal with the addition of WS_2 nanosheets and λ exonuclease. However, when FAM labeled dsDNA was reacted with both T4 PNK and λ exonuclease, a much lower fluorescence was observed. The fluorescence intensity of FAM labeled dsDNA catalyzed by T4 PNK and digested by λ exonuclease was 10 times smaller than that of FAM labeled dsDNA cleaved by λ exonuclease only. The main reason for this fact is that T4 PNK catalyzes the γ-phosphate residue of ATP transferring to the 5'-hydroxyl group of FAM labeled dsDNA, yielding a phosphate moiety at the 5'-dsDNA end. Also then λ exonuclease degrades FAM labeled dsDNA much more rapidly with 5'-phosphoral compared to the 5'-hydroxyl end. [29, 30] As a result, under the same reaction condition, FAM labeled dsDNA phosphorylated by T4 PNK was rapidly hydrolyzed by λ exonuclease, leaving fluorescent dye-labeled ssDNA, while FAM labeled dsDNA without 5'-phosphoral still remained unchanged. The different adsorption abilities of P1 and FAM labeled dsDNA on the WS_2 nanosheet surface lead to the significant discrepancy of the fluorescence signals. The results suggest that DNA phosphorylation is the rate determining step in the coupled enzymatic reaction system, and the accurate and rapid kinase activity measurement can be achieved through the T4 PNK-λ exonuclease system and the WS_2 nanosheets sensing platform.

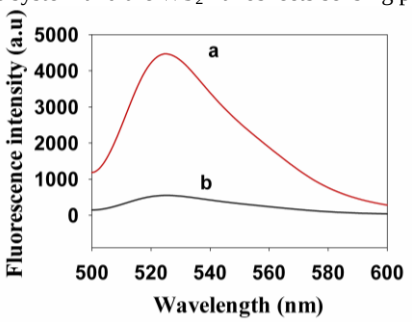

Fig. 3. Typical fluorescence spectra of 100 nM FAM labeled dsDNA without (a) and with (b) phosphorylation after addition of 20 μL of WS_2 nanosheets in the reaction buffer. The concentrations of ATP, λ exo, and T4 PNK were 0.5 mM, 10 units, and 10 U mL^{-1}, respectively.

Optimization of Sensing Conditions

It was found that the amount of WS_2 nanosheets used in the assay has substantial effect on the fluorescence quenching responses (Fig. S3 in ESI). The fluorescence responses in the presence of WS_2 nanosheets of different concentrations were examined. When P1 was mixed with WS_2 nanosheets, it adsorb onto the WS_2 nanosheet surface. It is obvious that the use of more WS_2 nanosheets leads to more efficient adsorption of P1, increasing the quenching efficiency. When concentration of WS_2 nanosheets is 5 μg mL^{-1}, the fluorescence signal of FAM labeled dsDNA relative to the fluorescence of FAM labeled ssDNA reaches the maximal value. Such observations could be ascribed to the weak adsorption of FAM labeled dsDNA on WS_2 nanosheet surfaces which became dominant in the presence of excessive WS_2 nanosheets. As a result, 5 μg mL^{-1} was used as the optimized concentration for WS_2 nanosheets.

In order to optimize the experimental conditions, a series of measurements were researched in this work. The time of phosphorylation is an important parameter for T4 PNK-catalyzed phosphorylation and the coupled λ exonuclease cleavage process. The fluorescence signal decreased gradually with the increase of the reaction time, and then reached equilibrium after 30 min, suggesting a complete phosphorylation and cleavage process (Fig. S4A in ESI). With further increase in the phosphorylation time, however, it did not weaken the currents response. This suggested that the phosphorylation reaction was completed less than 30 min. Thus, 30 min was chosen as the appropriate time in the following experiments.

The amount of λ exonuclease was also optimized to obtain sufficient digestion for T4 PNK assay. Obviously, as the amount of λ exonuclease increased, the fluorescence intensity decreased gradually (Fig. S4B in ESI). When the concentration of λ exonuclease was higher than 7.5 U, the intensity reached equilibrium. In order to obtain high effective digestion, 10U λ exonuclease was chosen in this work.

ATP acts as the enzymatic substrate and provides the phosphate group for 5'-hydroxyl dsDNA during the phosphorylation. Therefore, the influence of the concentration of ATP was examined (Fig. S4C in ESI). It could be seen that the concentration of ATP increased, the phosphorylation of the DNA resulted in the solution fluorescence intensity reaching its minimum at the ATP concentration of 0.5 mM. When the concentration of ATP was higher than 0.5 mM, the fluorescence signal increased again. This inhibition effect caused by higher concentrations of ATP on the phosphorylation process was probably due to a competitive binding reaction between the DNA and ATP. As a result, when the concentration of ATP was relatively high, the binding site of T4 PNK was partially blocked. Therefore, 0.5 mM was employed as the optimal ATP concentration to obtain a high sensitivity.

Detection of T4 PNK Activity

To evaluate the sensitivity of the WS_2 nanosheets-based sensor, we tested the response on different concentrations of T4 PNK based on the optimal assay conditions. Fig. 4A showed the fluorescence responses for different T4 PNK concentrations. It is observed that the fluorescence signals gradually decreased as the concentration of T4 PNK varied from 0.01 to 10 U mL^{-1}. The

amount of T4 PNK was reflected by the change of fluorescence signal, which originated from the FRET between fluorescent dye-labeled ssDNA and WS_2 nanosheets. Fig. 4B indicated the fluorescence signal was linearly decreased with the logarithm of T4 PNK concentration in the range from 0.01 to 10 U mL^{-1} (regression coefficient R^2 = 0.996). The relative standard deviations of peak fluorescence readings were 2.2%, 2.6%, 1.9% and 3.3% in three repetitive assays of 0.01 U mL^{-1}, 0.1 U mL^{-1}, 1 U $mL^{-1}$and 10 U mL^{-1} T4 PNK. The detection limit of T4 PNK was 0.01 U mL^{-1} according to the 3σ rule, which was lower than that of the previous ^{32}P-labeling methods (0.17 U mL^{-1}) [31] and comparable to the results obtained from reported assays.[13, 14, 32-34] The result indicated that the WS_2 nanosheet platform could be applied to sensitive kinase activity analysis in a wide concentration range.

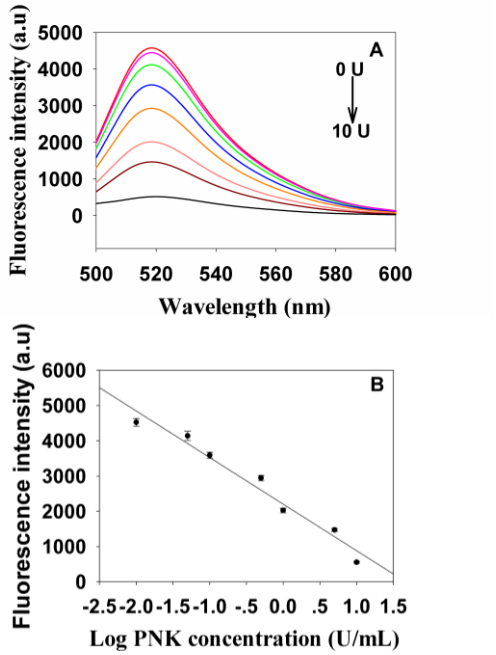

Fig. 4. (A) Fluorescence intensity_wavelength curves with different activity units of T4 PNK (top to bottom, 0, 0.01, 0.05, 0.1, 0.5, 1, 5, 10U mL^{-1}) in reaction buffer. (B) Calibration curve of WS_2 nanosheets nanosensor in the presence of increasing amount of T4 PNK dependence of fluorescence intensity on the logarithm of T4 PNK concentration . The concentrations of FAM labeled dsDNA, ATP, and λ exo were 100 nM, 0.5 mM, and 10 units, respectively. The error bars represented for standard deviation (SD) across three repetitive experiments.

Investigation of T4 PNK Activity Detection in Diluted Cell Extracts

The feasibility of the proposed strategy was also tested by the detection of T4 PNK in complex biological samples. In order to examine the possibility of the as-proposed sensing platform for cellular T4 PNK activity profiling, HeLa cell extracts were added in the buffer to simulate the intracellular environment during the test procedure. WS_2 nanosheets were found well dispersed in the reaction buffer containing 1% (v/v) cell extracts and no sediment was observed after 48 h. In the cell extracts-containing buffer, 20 μL of WS_2 were enough to quench 92% fluorescence emission of P1 (Fig. S5, curve d in ESI), while FAM labeled dsDNA still keeped 90% fluorescence intensity under the same conditions (Fig. S5, curve c in ESI). These phenomena are in good agreement with those in the reaction buffer without cell extracts. It is observed from Fig. 5A that the fluorescence signals decreased when the concentrations of T4 PNK gradually increased from 0.05 to 10 U mL^{-1}. The fluorescence intensity and the logarithm of T4 PNK concentration also exhibits a linear relationship like that operated in Tris-HCl buffer (Fig. 5B). The above results demonstrate that the as-proposed sensing platform works well in complex mixtures with other possible coexisting interfering specie, suggesting that the method could be further used for real sample analysis.

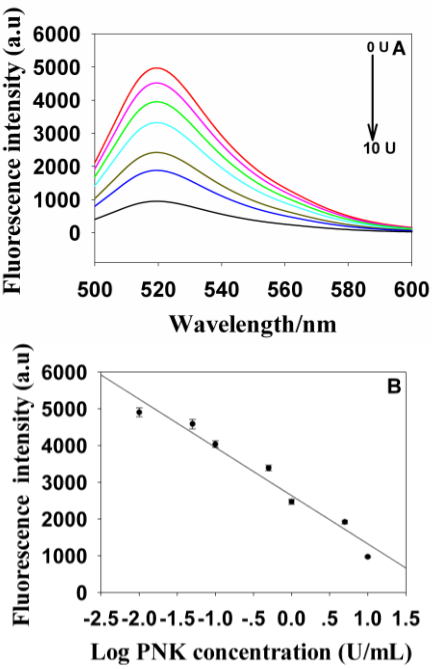

Fig. 5. (A) The fluorescence intensity with different activity units of T4 PNK in reaction buffer containing 1% (v/v) cell extracts. (B) The dependence of fluorescence intensity on the logarithm of T4 PNK concentration in reaction buffer containing 1% (v/v) cell extracts. The concentrations of FAM labeled dsDNA, ATP, and λ exo were 100 nM, 0.5 mM, and 10 units, respectively. The error bars represented for standard deviation (SD) across three repetitive experiments.

Assay Selectivity

To demonstrate the selectivity of the present strategy, control experiments using some nonspecific enzymes including lysozyme, PDGF-BB, APE 1, UDG and PKA were respectively tested with the procedures of T4 PNK assay and the same concentration of T4 PNK (10 U mL^{-1}). With the comparison of peak intensity after treatment by these enzymes, it was obviously observed that these nonspecific enzymes did not cause a remarkable fluorescence decrease, indicating a high selectivity of the proposed WS_2 nanosheets-based T4 PNK assay (Fig. S6 in ESI).

Assay of the Inhibition on T4 PNK Activity

To further extend the potential application of this method in the inhibition assay, WS_2 nanosheets-based nanosensor developed here could also be used for screening the inhibitors of T4 PNK. To evaluate this property, we investigated the inhibition effects of adenosine diphosphate (ADP), ammonium sulfate ($(NH_4)_2SO_4$),

and sodium chloride (NaCl) on the activity of T4 PNK. These chemicals are considered to have no inhibition effect on the activity of λ exonuclease,[13, 14, 35] thus, can be used as inhibitors for T4 PNK. From Fig. 6A the results clearly showed that with the increase of the assay solution ADP concentration, a gradual increase of fluorescence emission intensity was observed. The results indicate that the activity of T4 PNK became weaker with the increase of ADP concentration. The DNA phosphorylation was decreased by 50% when the ADP concentration was 1 mM. As expected, increasing concentrations of $(NH_4)_2SO_4$ also resulted in the increase of fluorescence intensity. Fig. 6B showed the amount of $(NH_4)_2SO_4$ causing a 50% DNA phosphorylation decrease was 15 mM. The effect of the two small molecules on T4 PNK activity is similar to that reported in literature.[13] Additionally, the inhibition effect on T4 PNK was also evaluated using NaCl, which has been confirmed that it could inhibit the T4 PNK activity by changing the affinity of the enzyme for its substrates.[14] Fig. 6C indicated the fluorescence intensity increased with the increase of NaCl concentration in the presence of T4 PNK, verifying the fluorescence increase was due to the inhibition effect of NaCl. All result suggests the potential use of the WS_2 nanosheets -based nanosensor for studies of T4 PNK inhibitors.

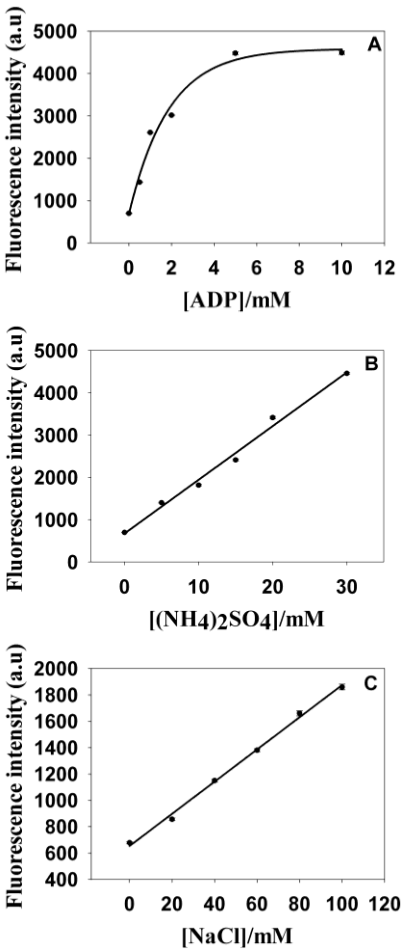

Fig. 6. Inhibition effects of (A) ADP, (B) $(NH_4)_2SO_4$, and (C) NaCl on phosphorylation. The assays were carried out in the reaction buffer, containing 100 nM FAM labeled dsDNA, 10 U mL^{-1} T4 PNK, 0.5 mM ATP, and 10 units λ exo. The error bars represented for standard deviation (SD) across three repetitive experiments.

Conclusions

In summary, the activity and its inhibitors of T4 PNK are sensitively and rapidly detected using the coupled λ exonuclease cleavage reaction and the WS_2 nanosheets-based sensing platform. The efficient cleavage capacity of λ exonuclease and the super quenching ability of WS_2 nanosheets both contribute to the sensitive screening of T4 PNK activity. The as-proposed method provides a wide linear range from 0.01 to 10 U mL^{-1} and a low detection limit of 0.01 U mL^{-1} for T4 PNK activity assay. In addition, this strategy is cost-effective and avoids the complex design of the hairpin DNA probe. Furthermore, the inhibition effects of ADP, $(NH_4)_2SO_4$, and NaCl on phosphorylation can be evaluated accurately and conveniently. Given the crucial roles of kinases in some biological processes, the sensitive and universal WS_2 nanosheets based sensing platform is not only provides a new platform for monitoring activity and inhibition of nucleotide kinase but also shows great potential in biological process researches, drug discovery, and clinic diagnostics.

Acknowledgement

This work was supported by the National Natural Science Foundation of China (No. 21275045, 21205034, 91317312), NCET-11-0121, Hunan Provincial Natural Science Foundation of China (Grant 12JJ1004, 13JJ4031), Doctoral Fund of Ministry of Education of China (New Teachers, 20120161120032), Fundamental Research Funds for the Central Universities and Young Scholar Support Program of Hunan University.

Notes and references

State Key Laboratory for Chemo/biosensing and Chemometrics, College of Chemistry and Chemical Engineering, Hunan University, Changsha, 410082, PR China. Tel.: +86 731 88821916; Fax: +86 731 88821916. E-mail address: xiachu@hnu.edu.cn, rqyu@hnu.edu.cn

1 C. Chappell, L.A. Hanakahi, F. Karimi-Busheri, M. Weinfeld, and S. C.West, *EMBO J*., 2002, **21**, 2827–2832.
2 C. J. Whitehouse, R. M. Taylor, A. Thistlethwaite, H. hang, F. Karimi-Busheri, D. D. Lasko, M. Weinfeld, and K. W. Caldecott, *Cell*, 2001, **104**, 107-117.
3 F. Chen, Y. X. Zhao, L. Qi, and C. H. Fan, *Biosens. Bioelectron*., 2013, **47**, 218-224.
4 C. C. Richards, *Proc. Natl. Acad. Sci. U.S.A*., 1965, **54**, 158−165.
5 A. Becker and J. J. Hurwitz, *Biol. Chem*., 1967, **242**, 936–950.
6 V. Cameron and O. C. Uhlenbeck, *Biochemistry*, 1977, **16,** 5120–5126.
7 D. H. Phillips and V. M. Arlt, *Nat. Protoc*., 2007, **2**, 2772–2781.
8 C. Frauendorf, F. Hausch, I. Rohl, A. Lichte, S. Vonhoff and S. Klussmann, *Nucleic Acids Res*., 2003, **31**, e34.
9 F. Karimi-Busheri, A. Rasouli-Nia, J. Allalunis-Turner and M. Weinfeld, *Cancer Res*., 2007, **67**, 6619–6625.
10 L. K. Wang, C.D. Lima and S. Shuman, *EMBO J*., 2002, **21**, 3873-3880.
11 N. K. Bernstein, R. S. Williams, M. L. Rakovszky, D.Cui, R. Green, F. Karimi-Busheri, R. S. Mani, S. Galicia, C. A. Koch, C. E. Cass, D. Durocher, M. Weinfeld, J. N. Glover, *Mol. Cell*., 2005, **17**, 657-670.
12 F. Karimi-Busheri, J. Lee, A. E. Tomkinson and M. Weinfeld, *Nucleic Acids Res*., 1998, **26**, 4395-4000.
13 Z. W. Tang, K. M. Wang, W. H. Tan, C. B. Ma, J. Li, L. F. Liu, Q. P. Guo and X. X. Meng, *Nucleic Acids Res*., 2005, **33**, e97.
14 C. Song and M. P. Zhao, *Anal. Chem*., 2009, **81**, 1383–1388.

15 X. Huang, X. Y. Qi, F. Boey and H. Zhang, *Chem. Soc. Rev*., 2012, **41**, 666-686.
16 Y. Wang, Z. H. Li, D. H. Hu, C. T. Lin, J. H. Li and Y. H. Lin, *J. Am. Chem. Soc*., 2010, **132**, 9274-9276.
17 L. H. Tang, Y. Wang, Y. Liu and J. H. Li, *ACS Nano*, 2011. **5**, 3817-3822.
18 B. W. Liu, Z. Y. Sun, X. Zhang and J. W. Liu, *Anal. Chem*., 2013, **85**, 7987-7993.
19 C. H. Lu, H. H. Yang, C. L. Zhu, X. Chen and G. N. Chen, *Angew. Chem., Int. Ed*., 2009, **48**, 4785-4787.
20 Y. S. Guo, X. P. Jia and S. S. Zhang, *Chem. Commun*., 2011, **47**, 725-727.
21 S. P. Song, Y. Qin, Y. He, Q. Huang, C. H. Fan and H. Y. Chen, *Chem. Soc. Rev.*, 2010, **39**, 4234-4243.
22 J. J. Xu, W. W. Zhao, S. P. Song, C. H. Fan and H. Y. Chen, *Chem. Soc. Rev.*, 2014, **43**, 1601-1611.
23 W. J. Zhao, Z. Ghorannevis, L. Q. Chu, M. L. Toh, C. Kloc, P. H. Tan and G. Eda, *ACS Nano*, 2013, **7**, 791-797.
24 M. Bernardi, M. Palummo and J. C. Grossman, *Nano Lett*., 2013, **13**, 3664-3670.
25 J. W. Liu and Y. Lu, *J. Am. Chem. Soc*., 2007, **129**, 9838-9839.
26 S. J. He, B. Song, D. Li, C. F. Zhu, W. P. Qi, Y. Q. Wen, L. H. Wang, S. P. Song, H. P. Fang and C. H. Fan, *Adv. Funct. Mater*., 2010, **20**, 453−459.
27 D. Voiry, H. Yamaguchi, J. W. Li, R. Silva, D. C. Alves, T. Fujita, M. W. Chen, T. Asefa, V. B. Shenoy, G. Eda and M. Chhowalla, *Nat. Mater*., 2013, **12**, 850-855.
28 M. D. Vodenicharov, F. R. Sallmann, M. S. Satoh and G. G. Poirier, *Nucleic Acids Res*., 2000, **28**, 3887-3896.
29 K. Subramanian, W. Rutvisuttinunt, W. Scott and R. S. Myers, *Nucleic Acids Res*., 2003, **31**, 1585–1596.
30 T. T. Perkins, R. V. Dalal, P. G. Mitsis and S. M. Block, *Science*, 2003, **301**, 1914–1918.
31 F. Karimi-Busheri, G. Daly, P. Robins, B. Canas, D. J. C. Pappin, J. Sgouros, G. G. Miller, H. Fakhrai, E. M. Davis, M. M. Le Beau and M. Weinfeld, *J. Biol. Chem*., 1999, **274**, 24187-24194.
32 L. Lin, Y. Liu, J. Yan, X. S. Wang and J. H. Li, *Anal. Chem*., 2013, **85**, 334-340.
33 C. J. Dobson and S. L. Allinson, *Nucleic Acids Res*., 2006, **34**, 2230-2237.
34 L. Lin, Y. Liu, X. Zhao and J. H. Li, *Anal. Chem*., 2011, **83**, 8396-8402.
35 R. S. Swathi and K. L. Sebastian, *J. Chem. Phys*., 2009, **130**, 086101.